

Estimating Peak Skin and Eye Lens Dose from Neuro-Perfusion Examinations Using
Monte Carlo Based Methods: Evaluation of the performances of CTDI_{vol}, TG111, and
IMPACT Dosimetry Tool

5

ABSTRACT

Purpose: CT neuro-perfusion examinations are capable of delivering high radiation dose to skin or lens of the eyes of the patient and could possibly cause deterministic effects.

10 The purpose of this study is to: (a) estimate dose from CT neuro-perfusion examinations to several voxelized adult patient models with slightly different head sizes and (b) investigate how well these doses can be approximated by some commonly used CT dose metrics or tools, such as $CTDI_{vol}$, TG111-like measurements, and the IMPACT dose calculator spreadsheet.

15 Methods: Monte Carlo simulation methods were used to estimate peak skin and eye lens dose on voxelized patient models, including GSF's Irene, Frank, Donna and Golem on four scanners from major manufacturers at the widest collimation under all available kVs. The doses were reported on a per 100 mAs basis. $CTDI_{vol}$ and TG111 peak dose measurements, as well as IMPACT calculations were performed for available scanners at
20 all kVs. These were then compared with results from Monte Carlo simulations.

Results: The dose variations across different patients are small. Depending on kV, the scanner and patient model, $CTDI_{vol}$ values overestimated peak skin dose by 26% to 65%, and overestimated eye lens dose by 33% to 106%. TG111-like measurements were much closer with peak skin estimates ranging from 14% underestimation to 33%
25 overestimation, and with eye lens dose estimates ranging from 9% underestimation to 66% overestimation. The IMPACT spreadsheet overestimated eye lens dose by 2% to 82%.

Conclusion: Radiation dose from CT neuro-perfusion examinations should be closely monitored. $CTDI_{vol}$ consistently overestimates dose to eye lens and skin. The IMPACT tool also overestimated dose to eye lenses. Therefore they can serve as conservative dose
30 estimators in CT neuro-perfusion studies. TG111-like measurements provide a better prediction to both peak skin and eye lens dose than $CTDI_{vol}$ and the IMPACT tool. It should be understood that both the TG111 peak dose metric and $CTDI_{vol}$ dose metric are still only indices, instead of actual patient doses.

35 **I. Introduction**

With the development of Multi-detector CT (MDCT) and increased computing power, CT perfusion imaging has become a common clinical examination used to explore the physiology of the cerebral vasculature, especially in the context of evaluating patients with a suspected stroke. Rather than the anatomical visualization of the morphology of discrete vessels, CT neuro-perfusion shows the functional status of the circulation of the cerebral blood and the perfusion of tissues. Therefore it is an essential non-invasive imaging method to depict the extent of cerebral ischemia for patients with stroke. Furthermore, it could rapidly provide information for the assessment to determine patient treatment and management options within a critical time window¹.

45 Because the radiation dose from routine head CT scans is relatively low (on the order of 10s of mGy), the stochastic effects have been regarded as the primary concern in terms of the biological consequences from radiation dose. However, in neuro-perfusion studies, the patient's head is scanned repeatedly at one location over a short period of time to monitor the wash in and wash out of iodinated contrast. This may result in very high radiation dose to skin and the eye lens and can lead to deterministic effects, such as erythema (skin burn) or epilation (hair loss), and high dose to the eye lenses may cause cataractogenesis, if the eye lenses are directly irradiated.

In order to investigate the radiation dose from neuro-perfusion CT scans, either retrospectively or prospectively, it is essential to have dose metrics that are easily measured and obtained. Currently CTDI is the most widely used dose metric for the estimation of radiation dose from CT and it is reported on all CT scanners and more recently in patient dose reports, such as shown in Figure 1. However CTDI is not patient dose², instead it represents the radiation dose to a homogeneous cylindrical phantom. In addition, the CTDI calculation assumes a contiguous set of scans over a relatively large region, and the measurements involve the use of a 100 mm long ion chamber, which approximates multiple scan average dose (MSAD) for scans with table incrementation. While this metric applies to many clinical uses of CT, in neuro-perfusion scans however, there is no table incrementation and local peak doses to skin and eye lens are of more interest. Therefore CTDI has been demonstrated to overestimate the peak skin dose³. It

65 may be more appropriate to use methods described in AAPM TaskGroup 111 report⁴,
where the measurements are performed at the 12:00 position of a 16cm diameter PMMA
phantom using a small ion chamber with a shorter active length in longitudinal direction
to estimate peak dose. Despite the fact that TG111 measurements could potentially
provide more accurate dose estimation to peak skin and eye lens dose, it still does not
70 take into account the complexity of the heterogeneity of patient's anatomy. The
IMPACT CT patient dosimetry calculator, a commonly used tool for CT dose purposes,
allows the users to select the scan range and reports simulated results based on Monte
Carlo methods. However, it matches the modern CT scanners with the original modeled
CT scanners using approximation methods instead of directly modeling the modern CT
75 scanners. Furthermore, it uses the MIRD mathematical patient model, in which all the
organs are represented by simple geometric shapes and also does not appreciate the
anatomical differences between patients. On the other hand, Monte Carlo based method
simulations using realistic voxelized patient models have been regarded and accepted as
the accurate method for estimation of radiation dose to individual organs⁵⁻¹³.

80 The local dose to skin tissue and eye lens from CT neuro-perfusion examinations should
be well understood so that potential radiation safety issues can be prevented. . Previous
work has investigated the peak skin dose and eye lens dose delivered to a patient during
CT neuro-perfusion scans for a range of scanning protocols¹⁴. The purpose of this study
is to: (a) extend the previous study and investigate dose to a variety of patients and (b)
85 investigate how well these doses can be approximated by some commonly used CT dose
metrics or tools, such as CTDI ,TG111 measurements, and IMPACT.

II. Methods and Materials

II. A CT Scanners Modeled

Four MDCT scanners, including a Siemens Sensation 64 scanner, a Toshiba Aquilion 64
90 scanner, a Philips Brilliance 64 scanner, and a GE LightSpeed VCT, were modeled to
represent a range of manufacturers. . The Siemens Sensation 64 (Siemens Healthcare,
Forchheim Germany) allows kVs of 80, 100, 120 and 140 and only offers one size bowtie
filter. The widest collimation for a neuroperfusion exam with this scanner is 24x1.2 mm

(28.8 mm total nominal beam width). The Toshiba Aquilion 64 (Toshiba Medical
95 Systems, Nasu Japan) offers kVs of 80, 100, 120 and 135; this scanner employs three
different bowtie filters but adult head scanning primarily uses the small sized bowtie,
which was used in these simulations. The widest collimation for a neuroperfusion exam
with this scanner is 64x0.5 mm (32 mm total nominal beam width). The Philips Brilliance
64 (Philips Healthcare, Cleveland, OH) allows kVs of 80, 120 and 140 and only offers
100 one size bowtie filter. The widest collimation for a neuroperfusion exam with this scanner
is 32x1.25mm (40 mm total nominal beam width). The GE VCT (GE Healthcare,
Waukesha, WI) offers kVs of 80, 100, 120 and 140, this scanner also employs three
different bowtie filters but adult head scanning primarily uses the medium sized bowtie,
which was used in the simulations. The widest collimation for a neuroperfusion exam
105 with this scanner is 64x0.625 mm (40 mm total nominal beam width).

II.B. Monte Carlo Simulation Tools for CT scanners

MCNPX (MCNP eXtended v2.6), a Monte Carlo method based software package
developed at Los Alamos National Laboratory, was used for all the simulations in this
study. The simulations were performed in photon mode (assuming charged-particle
110 equilibrium) with a cutoff energy of 1keV. MCNPX source code (file source.f) was
modified to allow sophisticated source inputs for CT scanners, including the information
of spectrum, bowtie filter, table feed, collimation, scan start location, scan length and so
on^{7,8}. In order to get the information of spectrum and bowtie filter, a previously
developed methodology was used in this study to construct equivalent sources. The
115 equivalent source method uses data that can be obtained from scanner measurements
(including Half Value Layer, Quarter Value Layer and bowtie profile measurements) to
generate equivalent spectrum and bowtie to create CT source models for Monte Carlo
simulations¹⁵. As stated above, four scanner models from major manufacturers were
created using this method, including a Siemens Sensation 64 scanner, a Toshiba Aquilion
120 64 scanner, a Philips Brilliance 64 scanner, and a GE LightSpeed VCT scanner. These
models were benchmarked with measurements in CTDI body and head phantoms at both
center and 12:00 and they agreed to within 5%¹⁵.

II.C. Patient models

The GSF (now: Helmholtz Zentrum München) voxelized phantoms are a series of patient
125 phantoms with segmented individual organs and tissues¹⁶. Of specific interest for this
study was that both skin and lens of the eye were explicitly represented in these patient
models and so radiation dose could be tallied in these voxels. Because neuro-perfusion
examinations are rarely performed on pediatric patients, only adult patients were
considered in this study. Two adult male and two adult female patient models (Irene,
130 Donna, Golem, and Frank) were selected to represent a reasonable adult patient cohort.
As shown in Table I, although these four patient models have various body habitus, their
head sizes are very similar. Since in neuro-perfusion scans the head is the only body part
exposed to radiation, these four models represent the variation of patient anatomy, rather
than the variation of patient body size. The elemental composition and mass density of
135 each organ are required in order to incorporate each phantom into the MCNPX for
simulation. The ICRU 44 organ composition tables were used to derive these values¹⁷.

II.D. Scanning Protocol

For each combination of the four patient models and the four scanner models, all
available kVs were simulated and the doses were reported on a per 100mAs basis. We
140 realize that appropriate scanning techniques would involve the adjustment of mAs as kV
is changed, but the results provided here are easily scalable by the actual mAs used for a
given scanner and kV setting. As in the previous study¹⁴, to represent a worst case
scenario the scan simulations were performed using repeated axial scans at the location
where the primary beam covers the eye lens completely. .

145 The widest collimation and typical bowtie filter for head scan was used for each scanner.
It should be noted that although the highest tube voltage setting (140kV or 135kV) is not
usually used for brain perfusion scans in clinical protocols, the results could still serve as
a reference.

II.E. estimation of peak skin dose and eye lens dose

150 By defining the tally voxels at various locations, the radiation dose can be assessed
anywhere in the patient models using MCNPX. In order to get the peak dose for skin, the
mesh tally feature in MCNPX was used to get 3D dose distribution in the patient model

within the scan range. Mesh tallies are composed of a 3D array of voxels in a high-resolution Cartesian-coordinate mesh structure. These mesh tally voxels were set to overlap perfectly with the voxels making up the the patient phantom.

Since the mesh tally result is a 1D array representing a 3D dose distribution, it does not directly distinguish between different tissues and so further processing is required. In order to identify the skin tissue and eye lens tissue, a MATLAB subroutine was created to map the original patient model matrix to the 3D dose distribution matrix from mesh tally. The peak skin dose and eye lens dose were then obtained as the maximum dose and the average dose of those voxels identified as belonging to the skin and eye lens, respectively. The dose results were first divided by the density of the skin or eye lens to convert the unit from MeV/cm³/particle to MeV/g/particle, then it was multiplied by the normalization factors to get absolute dose. The normalization factors were calculated from scan measurements in air at isocenter and corresponding simulations in air at isocenter, described in previous publications^{7,8}.

II.F. Comparison of Estimated Peak Doses to Measurements and IMPACT calculations

In order to investigate how well CTDI and TG111 measurements predict the peak dose of eye lens and skin, these values were obtained by measurements on the scanners. To obtain CTDI_{vol} values, standard CTDI head measurements (single axial scan with a 100mm long pencil ion chamber in a 16 cm diameter PMMA CTDI head phantom) were performed using the same collimation and bowtie settings for all four scanners investigated in this study under all available tube voltage. Then CTDI_{vol} values under each condition were calculated by the weighted summation of CTDI at 12:00 position and CTDI at center position¹⁸. For most scanners, there is a small difference between the CTDI value at the 12:00 position and that at center position, so for this work, we chose the CTDI_{vol} value which is reported by the scanner. [MK1]

For TG111 measurements, single axial scans were also performed and readings from the 12:00 position of a CTDI head phantom were obtained using a small (0.6 cc) ionization chamber (Model 10X5-0.6CT, Radcal Corporation , Duarte, CA); this chamber has an active length of approximately 20mm. Due to limited access to all scanners, TG111 small

chamber measurements were performed under all kVs for the Siemens Sensation 64 scanner, the GE LightSpeed VCT scanner, and the Toshiba Aquilion 64 scanner.

185 Eye lens dose was obtained for each kV setting for all four scanners from IMPACT (version 1.0.3) on a per 100 mAs basis. IMPACT only reports the average dose to skin instead of local peak skin dose, therefore only eye lens doses were compared between Monte Carlo simulations and IMPACT. The scan range was selected so that the eye lens is fully covered by the primary beam, which is the scenario in the simulations. This is illustrated in Figure 2.

190 **III. Results**

III.A. Peak radiation dose to skin and eye lens for different scanners and patients

Peak skin dose and eye lens dose were calculated in the unit of milli-Gray (mGy) on a per 100 mAs basis for each kV on all four scanners for all four patients, as shown in Table II. It was also graphically plotted in Figure 3. The abscissa of Figure 3 is the combination of
195 different scanners and patient models, while the ordinate is the radiation dose for different kVs. As shown in Figure 3, peak skin dose is almost always a little higher than eye lens dose under the same condition, but the behavior of peak skin dose and eye lens dose across different kV, different scanners and different patient models are very similar. Depending on the scanner, kV and patient model, the peak dose to skin from a single
200 neuro-perfusion [MK2]examination ranges from 2.3 mGy/100mAs to 18.2 mGy/100mAs. For example, peak skin dose for Irene at 80kV from Philips Brilliance 64 is 2.3 mGy/100mAs, while the peak skin dose for Irene at 140kV from GE LightSpeed VCT is 18.2 mGy/100mAs. Meanwhile, the peak dose to eye lens ranges from 2.0 mGy/100mAs to 16.2 mGy/100mAs. For example, eye lens dose for Donna at 80kV from Philips
205 Brilliance 64 is 2.0 mGy/100mAs, while the eye lens dose for Golem at 135kV from Toshiba Aquilion is 16.2 mGy/100mAs. It should be noted that 140kV is not usually used in clinical practice for neuro-perfusion exams; these values are primarily shown for comparisons.

The effect of technical parameters (here kV) can be significant. Higher kV always results
210 in higher dose when the same mAs were used. For example, peak skin dose per 100 mAs

at 120kV is always about 2 to 3 times higher than that at 80kV across all the scanners and patient models.

The dose difference across various scanners can also be significant and is up to a factor of two for the sample of scanners used in this study, which is consistent with previously published work¹⁹. For example, for patient Donna at 120 kV, the peak skin dose from Toshiba Aquilion 64 is 14.2 mGy/100mAs, while it is 7.3 mGy/100mAs from Philips Brilliance 64. This shows that a factor of two difference can exist between two different scanners, even using the same kV and mAs settings.

The dose difference across the various patients for a specific scanner is fairly small. For example, for Siemens Sensation at 80 kV, the peak skin dose ranges from 2.8 mGy/100mAs to 3.0 mGy/100mAs among all four patient models investigated in this study. These small differences between patients were observed across scanners and kVs.

III.B. Computation time

All the simulations were performed on a parallel computing cluster server with 32 AMD 2.0 GHz processors. The number of particles (NPS) in MCNPX was set to 100 million to ensure good statistics. The mesh tally used in this study caused prolonged running time because all the photon interactions happened in each mesh tally voxel had to be tracked. The average running time for each simulation is about 5 hours. The error of all the results from mesh tally was within 1%.

III.C. Performance of $CTDI_{vol}$ measurements to predict peak skin and eye lens dose

Table III shows the $CTDI_{vol}$ measurements that were obtained at corresponding bowtie filtration and collimation settings under all available kVs on the four scanners modeled in this study. As was done for the simulated peak doses, these values were also normalized on a mGy/100mAs basis. Figure 4a shows the ratio of $CTDI_{vol}$ to peak skin dose, while Figure 4b shows the ratio of $CTDI_{vol}$ to eye lens dose, for all kVs, all scanners and all patient models. Ratios higher than one mean overestimation, while ratios lower than one indicate underestimation.

Figure 4 shows that $CTDI_{vol}$ generally overestimates peak dose to both skin and eye lens. Depending on kV, the scanner and patient model, $CTDI_{vol}$ can overestimate peak skin
240 dose by 26% to 65%, with the average overestimation of 44%, and it overestimates eye lens dose by 33% to 106%, with the average overestimation of 67%. $CTDI_{vol}$ overestimates eye lens dose more than peak skin dose because eye lens dose is usually a little lower than skin dose, as shown in Figure 3.

III.D. Performance of TG111 measurements to predict peak skin and eye lens dose

245 Table IV shows the results of the TG111 measurements that were performed for three of the four scanners modeled in this study under all kV conditions. Figure 5a and Figure 5b show the ratio of TG111 measurements to peak skin dose and eye lens dose, respectively. As in the previous section, the ratios higher than one mean overestimation, while ratios lower than one indicate underestimation. As previously mentioned in section II.F and
250 noted in Table IV, TG111 measurements were only performed for three of the four scanners so Figure 5 has less data points. Figure 5 shows that TG111 measurements provide a better prediction to both peak skin and eye lens dose than $CTDI_{vol}$ does. Depending on kV, scanner and patient model, TG111 measurements predict the skin dose from 14% underestimation to 33% overestimation, with the average prediction across all
255 kVs, scanner and patient models of 7% overestimation. For eye lens dose, the TG 111 measured values predict the eye lens dose from 9% underestimation to 66% overestimation, with the average prediction of 27% overestimation.

III.E. Performance of IMPACT calculations to predict eye lens dose

Table V shows the IMPACT calculations for eye lens dose under each condition. Figure
260 6 shows the ratios of IMPACT calculations of eye lens dose to the simulated eye lens dose using Monte Carlo methods. This figure demonstrates that IMPACT calculations also overestimate eye lens doses in most of the cases. Depending on the kV, the scanner and patient model, the overestimation can vary from 2% to 82%. The average overestimation is 43%.

265 **IV. Discussion and Conclusion**

This study used Monte Carlo method based simulations and provided estimations to peak skin dose and eye lens dose from CT neuro-perfusion scans for a range of adult patients under different tube voltage settings for four scanners from major manufacturers. Several dose metrics, including the widely used $CTDI_{vol}$ and the newly proposed TG111
270 measurements, as well as IMPACT, a commonly used CT dose tool, were used in this study. Their performances were evaluated as to how well they approximate the Monte Carlo estimated peak skin and eye lens doses.

Figure 3 demonstrates dose to skin and eye lens at all kVs on different scanners for different patients. By comparing the dose difference across kV (each column of data
275 points), it was shown that at the same mAs, higher kV always yields higher organ dose. This is because the x-ray intensity is approximately proportional to the square of tube voltage, and there is larger amount of photons coming out of the x-ray tube at a higher kV, even at the same mAs.

By comparing the dose difference across patients, it was shown that the dose variation
280 between patients is very small. This is not consistent with other studies that report higher doses for smaller patients⁹, because the body part of interest in this study is head, which does not vary much among adult patients. These results also indicate that the anatomical variation between adult patients is not very large. The morphologies of both skin and eye lens are reasonably constant across patients: they are both organs located at surface and
285 have little shielding effect from surrounding organs.

On the other hand, by comparing the dose difference across scanners, it was shown that there is substantial dose variation between the scanners. This is consistent with previous work which studied the doses to different organs in abdominal region and also showed large dose differences¹⁹. This is primarily because of differences in filtration (including
290 bowtie composition, thickness and shape) among various CT scanners. However, one cannot assert the superiority of one scanner over another solely based on the dose information because the image quality from these scanners can be different and is not considered here.

The results reported here can be used to estimate the peak skin dose and eye lens dose
295 from brain perfusion scans for an arbitrary protocol using any of the four CT scanners
simulated in the study. For example, as illustrated in a previous study¹⁴, the skin dose
from AAPM recommended protocol for model Irene ranges from 87 mGy to 348 mGy,
and the eye lens dose from AAPM recommended protocol for model Irene ranges from
81 mGy to 279 mGy (AJR paper).

300 The results of this study showed that $CTDI_{vol}$ overestimates peak skin dose by 26% to
65%, and it overestimates eye lens dose by 33% to 106%. This is primarily because of the
integration of the 100cm long ion chamber in the $CTDI_{vol}$ measurement. It captures (most
of) the scatter tails of the longitudinal radiation profile within the length of the 100 cm
ion chamber and estimates the average dose to the active volume in the chamber. On the
305 other hand, peak dose obviously refers to a concept of local dose and does not account for
the integration.

This motivated us to investigate TG111 approach which uses a small chamber and
provides closer values to a peak dose measurement. Our study shows that it does provide
a closer estimate to both eye lens and peak skin dose. For example, TG111 predicts the
310 skin dose from 14% underestimation to 33% overestimation, and it predicts the eye lens
dose from 9% underestimation to 66% overestimation. However, it should be noted that
if the collimation is narrower than the active length of the small chamber (approximately
20 mm), partial volume correction would be needed; this was not the condition in this
study where all collimations exceeded 24 mm, but it may be possible in another situation.

315 The IMPACT CT dosimetry tool was shown to overestimate the eye lens dose by 2% to
82%. This may be due to IMPACT using approximation methods to match the old
scanner CT models to the modern CT scanner (based on $CTDI_{vol}$ values) as well as using
a geometric patient model, including the eye. It was not possible to estimate peak skin
dose using the IMPACT CT dose tool as it only reports the average to the entire skin.

320 Overall, $CTDI_{vol}$ does provide a very conservative estimate (over by at least 30%) of peak
skin and eye lens dose. Though there is underestimation in some scenarios, predictions
using TG 111 measurements provide values that are closer to the simulated values for

both eye lens and skin dose. However, physicists and physicians should be aware that it still does not represent patient dose.

325 The relative values in Figure 4 and Figure 5 ($CTDI_{vol}/\text{peak dose}$) were shown to be much closer to each other than those in Figure 3 (peak dose), both across different kV within one scanner and across different scanners. This demonstrates that both $CTDI_{vol}$ and TG111 measurements do a reasonably good job of taking into account the spectra variations across both kV and scanners.

330 It is meaningful to compare these results in three different aspects. First, for a specific scanner and patient model combination, the differences between these relative dose values ($CTDI_{vol}/\text{peak dose}$) across kVs are small. For example, the points representing different kVs in Figure 4 and Figure 5 almost perfectly overlap with each other. This indicates that both CTDI and TG111 dose metrics take into account the changes of the
335 photon energy spectra; when a different kV is used, the behaviors of these two metrics are consistent with the behavior of the actual organ doses. Therefore the ratios are almost the same at different kVs. Second, for one specific scanner but different patient models, the estimation values do not vary much because the organ doses do not vary much across patients, as described previously. Third, there are some differences among estimated
340 values from different scanners. For example, for Donna at 80 kV, the CTDI overestimation of skin dose is 33% on Siemens Sensation 64 scanner, 45% on GE LightSpeed VCT scanner, 43% on Philips Brilliance 64 scanner, and 28% on Toshiba Aquilion 64 scanner. These results seem to be inconsistent with another previously published work where organ dose from helical scans on different scanners were
345 normalized by their $CTDI_{vol}$ and the normalized results were very close, thus suggesting the feasibility to use the same coefficients to convert $CTDI_{vol}$ to organ dose even for different scanners¹⁹. The context is a little different in these two studies. In the study by Turner et al helical scans were used, therefore each organ not only receives dose from the primary beam, but also receive scatters from adjacent tube rotations. This is naturally
350 equivalent to the intrinsic property of CTDI measurement, where both primary beam and scatter tails were included in the measured dose. In this study however, axial scans with no table motion were used and peak dose was of interest, where there is no scatter from

adjacent rotations. Since the results at different kVs have already shown that the photon spectra differences are well taken into account by $CTDI_{vol}$, the differences of $CTDI_{vol}$ performances among these four scanners could be from different bowtie design, geometry and collimations.

Although TG111 measurements were only performed for three scanners, Figure 5 showed that its performance is also not very consistent across these three scanners. For example, for Siemens Sensation 64 scanner and Toshiba Aquilion 64 scanner, TG111 measurements are very close to peak skin dose while for GE LightSpeed VCT scanner, TG111 measurements give about 30% overestimation. Since there is no additional scatter from adjacent rotations in TG111 measurements, this dose metric should theoretically provide a more accurate estimate to point dose. The fact that it overestimates peak dose for GE LightSpeed VCT scanner is probably because of the scanner geometry and the shape of the bowtie filter.

There are several limitations in this study. First, it did not model a recently developed technique (volume shuttle mode) utilized in some new scanner models (e.g. GE Discovery 750HD scanner, Siemens Definition Flash scanner) during neuro-perfusion examinations. While this new technique may spread the total dose to a larger volume of the patient's anatomy, it may not necessarily reduce the peak dose, if there is still some overlap between the two beams at extremity positions, so that certain part of the anatomy is always irradiated. Second, the sample size of the patient models is not very large. While the four GSF patient models used in study represent a distribution of patient habitus, they cannot represent the entire patient population.

Furthermore, the recently developed ICRP phantoms (ICRP 110) were not used in the study²⁰. While these phantoms have higher spatial resolution and may yield more accurate results, previous publication has demonstrated that the simulated organ dose results were within 1% between the 256 x 256 and 128 x 128 axial simulation matrix (DeMarco 2007). Therefore the results from the new ICRP phantoms are not expected to be significantly different than the results from this study. In addition, usually patients with smaller size receive higher organ dose when the same scanning technique is used^{9,11,12,21}. However, only small differences of peak skin and eye lens dose were

observed in this study because this study focuses specifically on the patient head region, where there is only small variation in terms of the head size for adult patients. Pediatric patients may receive higher organ doses for the same scanning protocol, but brain perfusion examinations are mostly for adult patients in clinic and hence adult patients are more relevant. [MK3] Third, tube current modulation (TCM) was not explicitly modeled in this study and all the simulations were performed at fixed tube current. Because of the non-uniformity of the attenuation of patient body across different projection angles, the photon flux reaching detectors is also not uniform. Therefore TCM is often suggested to be employed in CT scans to match photon flux on the detectors and therefore reduce excessive radiation dose²²⁻²⁴. But in neuro-perfusion examinations, TCM does not modulate tube current too much because of the relatively circular shape of head. In fact, it is often not used in these examinations and the AAPM CT protocols for neuro-perfusion recommend against using it “as it may interfere with the calculation of the BV and BF parameters”²⁵.

In summary, radiation dose from CT neuro-perfusion examinations should be closely monitored. These include the accurate estimation of radiation dose (including the prospective prediction of dose and the retrospective evaluation of dose), the reduction of dose (for example, tilting the gantry or avoiding direct exposure to eye lenses in order to reduce eye lens dose¹⁴), the optimization of scan protocol, the enforcement of optimized scan protocol and the elimination of operator errors. This study could facilitate the optimization of scan protocol by providing very detailed dose perspectives across different patients and scanner models. In addition, it was demonstrated that TG111 measurements estimate peak skin and eye lens dose closer than both $CTDI_{vol}$ values and results from the IMPACT CT dosimetry tool. While Task Group Report 111 was only recently published and these measurements are still not widely standardized, $CTDI_{vol}$ reported on the scanner can still serve as a conservative estimation of the peak doses. However, one should be aware that both TG111 peak dose metric and $CTDI_{vol}$ dose metric are still only indices, instead of actual patient dose

1. Miles, K., Eastwood, J.D. & König, M. *Multidetector computed tomography in cerebrovascular disease : CT perfusion imaging*, (Informa Healthcare, Abingdon, Oxon, 2007).
- 415 2. McCollough, C.H., S.Leng & et.al. CT Dose index(CTDI) and patient dose: they are not the same thing. *Radiology* **259**, 311-316 (2011).
3. Bauhs, J.A., Vrieze, T.J., Primak, A.N., Bruesewitz, M.R. & McCollough, C.H. CT dosimetry: comparison of measurement techniques and devices. *Radiographics* **28**, 245-253 (2008).
- 420 4. AAPM. Comprehensive Methodology for the Evaluation of Radiation Dose in X-Ray Computed Tomography. *AAPM report NO. 111* (2010).
5. DeMarco, J.J., Solberg, T.D. & Smathers, J.B. A CT-based Monte Carlo simulation tool for dosimetry planning and analysis. *Medical Physics* **25**, 1-11 (1998).
6. Zankl, M., Fill, U., Petoussi-Henss, N. & Regulla, D. Organ dose conversion coefficients for external photon irradiation of male and female voxel models. *Physics in Medicine and Biology*, 2367 (2002).
- 425 7. Jarry, G., DeMarco, J.J., Beifuss, U., Cagnon, C.H. & McNitt-Gray, M.F. A Monte Carlo-based method to estimate radiation dose from spiral CT: from phantom testing to patient-specific models. *Physics in Medicine and Biology*, 2645 (2003).
8. DeMarco, J.J., et al. A Monte Carlo based method to estimate radiation dose from multidetector CT (MDCT): cylindrical and anthropomorphic phantoms. *Physics in Medicine and Biology*, 3989 (2005).
- 430 9. DeMarco, J.J., et al. Estimating radiation doses from multidetector CT using Monte Carlo simulations: effects of different size voxelized patient models on magnitudes of organ and effective dose. *Physics in Medicine and Biology*, 2583 (2007).
- 435 10. Angel, E., et al. Radiation Dose to the Fetus for Pregnant Patients Undergoing Multidetector CT Imaging: Monte Carlo Simulations Estimating Fetal Dose for a Range of Gestational Age and Patient Size. *Radiology* **249**, 220-227 (2008).
11. Angel, E., et al. Monte Carlo simulations to assess the effects of tube current modulation on breast dose for multidetector CT. *Physics in Medicine and Biology*, 497 (2009).
- 440 12. Lee, C., et al. Organ and effective doses in pediatric patients undergoing helical multislice computed tomography examination. *Medical Physics* **34**, 1858-1873 (2007).
13. Perisinakis, K., Tzedakis, A. & Damilakis, J. On the use of Monte Carlo-derived dosimetric data in the estimation of patient dose from CT examinations. *Medical Physics* **35**, 2018-2028 (2008).
- 445 14. Zhang, D., et al. Peak skin and eye lens radiation dose from brain perfusion CT based on Monte Carlo simulation. *AJR Am J Roentgenol* **198**, 412-417 (2012).
15. Turner, A.C., et al. A method to generate equivalent energy spectra and filtration models based on measurement for multidetector CT Monte Carlo dosimetry simulations. *Medical Physics* **36**, 2154-2164 (2009).
- 450 16. Petoussi-Henss, N., Zankl, M., Fill, U. & Regulla, D. The GSF family of voxel phantoms. *Physics in Medicine and Biology*, 89 (2002).
17. ICRU. Tissue Substitutes in Radiation Dosimetry and Measurement. *ICRU Report No. 44* (1989).
18. McNitt-Gray, M.F. AAPM/RSNA Physics Tutorial for Residents: Topics in CT. Radiation dose in CT. *Radiographics* **22**, 1541-1553 (2002).
- 455 19. Turner, A.C., et al. The feasibility of a scanner-independent technique to estimate organ dose from MDCT scans: using CTDIvol to account for differences between scanners. *Med Phys* **37**, 1816-1825 (2010).

- 460 20. Adult Reference Computational Phantoms, ICRP Publication 110 Ann. *ICRP* 39 (2),
<http://www.icrp.org/publication.asp?id=ICRP%20Publication%20110> (2009).
21. AAPM. Size-Specific Dose Estimates (SSDE) in Pediatric and Adult Body CT Examinations.
AAPM report No. 204 (2011).
22. Gies, M., Kalender, W.A., Wolf, H. & Suess, C. Dose reduction in CT by anatomically
adapted tube current modulation. I. Simulation studies. *Med Phys* **26**, 2235-2247 (1999).
- 465 23. Kalender, W.A., Wolf, H. & Suess, C. Dose reduction in CT by anatomically adapted tube
current modulation. II. Phantom measurements. *Med Phys* **26**, 2248-2253 (1999).
24. Greess, H., *et al.* Dose reduction in computed tomography by attenuation-based on-line
modulation of tube current: evaluation of six anatomical regions. *Eur Radiol* **10**, 391-394
(2000).
- 470 25. AAPM. <http://www.aapm.org/pubs/CTProtocols/documents/AdultBrainPerfusionCT.pdf>.
(2010).

475 Table I. Age, gender, and size descriptions of the 4 patient models used in this study.

Model	Age	Gender	Weight	Height	Head perimeter
	(yr)		(kg)	(cm)	(mm)
Golem	38	Male	69	176	61
Frank	48	Male	95	174	61
480 Irene	32	Female	51	163	57
Donna	40	Female	79	170	56

TABLE II. Peak skin dose and eye lens dose from Monte Carlo neuro-perfusion simulations for four patient models under all kVs on four CT scanners. The doses were normalized on a mGy per 100 mAs basis. a) Peak skin dose; b) Eye lens dose.

a) Peak skin dose

kV	Siemens Sensation 64 (mGy/100mAs)				GE VCT (medium bowtie) (mGy/100mAs)				Philips Brilliance 64 (mGy/100mAs)				Toshiba Aquilion 64 (small bowtie) (mGy/100mAs)			
	Irene	Frank	Donna	Golem	Irene	Frank	Donna	Golem	Irene	Frank	Donna	Golem	Irene	Frank	Donna	Golem
80kV	3.0	2.8	3.0	2.8	5.2	5.0	5.2	4.9	2.3	2.4	2.3	2.4	5.4	5.3	5.4	5.2
100kV	6.2	6.1	6.3	5.9	8.8	8.5	8.8	8.3					9.5	9.2	9.5	9.0
120kV	10.5	10.3	10.5	10.0	13.2	12.8	13.1	12.4	7.2	7.5	7.3	7.3	14.1	13.8	14.2	13.4
140kV (135 for Aquilion)	16.4	16.5	16.5	16.0	18.2	17.5	18.1	17.0	11.1	11.6	11.1	11.2	18.1	17.6	18.1	17.1

485

b) Eye lens dose

kV	Siemens Sensation 64 (mGy/100mAs)				GE VCT (medium bowtie) (mGy/100mAs)				Philips Brilliance 64 (mGy/100mAs)				Toshiba Aquilion 64 (small bowtie) (mGy/100mAs)			
	Irene	Frank	Donna	Golem	Irene	Frank	Donna	Golem	Irene	Frank	Donna	Golem	Irene	Frank	Donna	Golem
80kV	2.5	2.5	2.2	2.6	4.1	4.3	3.8	4.6	2.2	2.1	2.0	2.3	4.4	4.6	4.0	4.8
100kV	5.4	5.4	4.8	5.6	7.1	7.5	6.6	7.8					7.7	8.2	7.1	8.5
120kV	9.3	9.3	8.4	9.6	10.7	11.4	9.9	11.8	6.7	6.8	6.2	7.1	11.5	12.3	10.6	12.7
140kV (135 for Aquilion)	15.0	15.0	13.8	15.6	14.7	15.7	13.6	16.1	10.4	10.4	9.8	11.0	14.7	15.8	13.6	16.2

490 TABLE III. CTDI_{vol} measurements for all kVs on four scanners modeled in this study. The values were normalized on a mGy per 100 mAs basis.

	Siemens Sensation 64	GE VCT (medium bowtie)	Philips Brilliance 64	Toshiba Aquilion 64 (small bowtie)
80kV	4.0	7.5	3.3	6.9
100kV	8.3	13.3		13.2
120kV	13.7	20.2	11.1	19.9
140kV (135 for Aquilion)	20.9	28.0	16.1	26.5

TABLE IV. TG111 measurements for all kVs on three of the four scanners modeled in this study. The values were normalized on a mGy per 100 mAs basis.

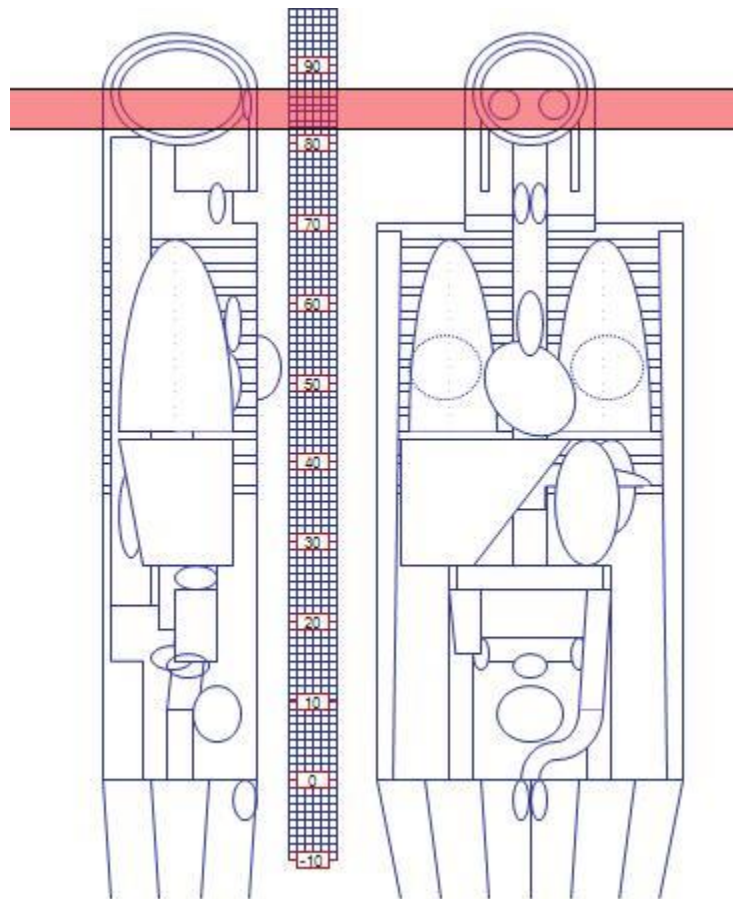
	Siemens Sensation 64	GE VCT (medium bowtie)	Toshiba Aquilion 64 (small bowtie)
80kV	2.8	6.3	5.4
100kV	5.6	10.9	9.4
120kV	9.4	16.5	14.8
140kV (135 for Aquilion)	14.2	22.6	19.1

495 TABLE V. IMPACT eye lens dose calculations for all kVs on four scanners modeled in this study. The values were normalized on a mGy per 100 mAs basis.

	Siemens Sensation 64	GE VCT (medium bowtie)	Philips Brilliance 64	Toshiba Aquilion 64 (small bowtie)
80kV	3.3	6.7	3.2	5.7
100kV	6.6	12.0		12.0
120kV	11.0	18.0	9.9	17.0
140kV (135 for Aquilion)	16.0	24.0	13.0	23.0

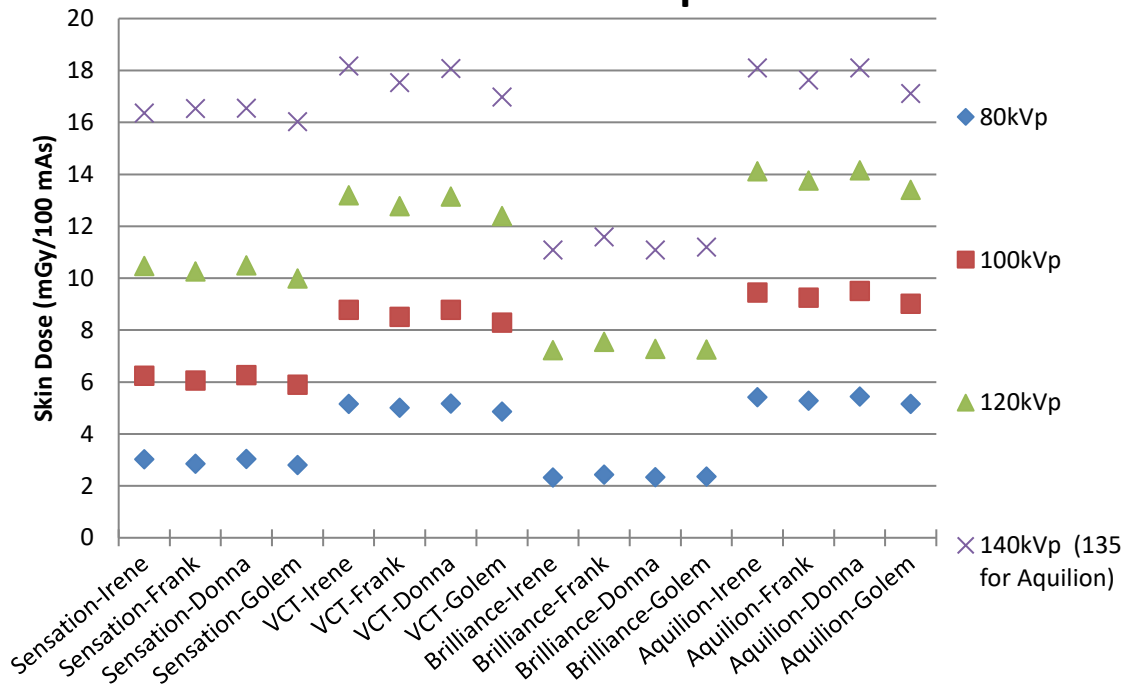
Total mAs 9229		Total DLP 3244 mGycm					
	Scan	kV	mAs / ref.	CTDI _{vol} mGy	DLP mGycm	TI s	cSL mm
Patient Position H-SP							
Head/NETopo	1	120	35 mA			4.2	0.6
HdSeq XC wo	2	120	214 / 240	37.08	640	2.0	1.2
Perfusion w	7	80	95	211.86	814	1.0	1.2
PreMonitoring	8	120	20	2.44	2	0.5	10.0
Contrast							
Monitoring	9	120	20	19.53	20	0.5	10.0
CTA Brain/Nck	17	120	308 / 335	43.39	1768	0.5	0.6

500 **Figure 1. An example of a dose report for a brain perfusion scan showing CTDI_{vol} and DLP values for each individual scan series.**



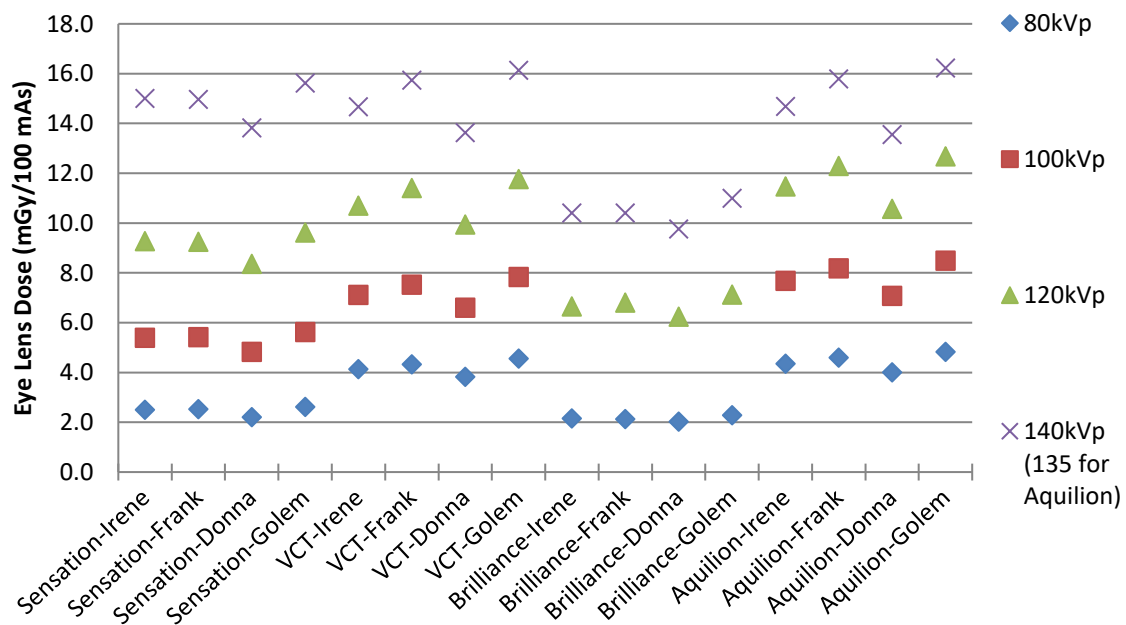
505 **Figure 2. The mathematical phantom in IMPACT for the calculation of eye lens dose. The pink region shows a scan range from z=82 to z=87 which completely covers the eye lens.**

Skin dose under each kVp on all four scanners for all four patients



(a)

Eye lens dose under each kVp on all four scanners for all four patients

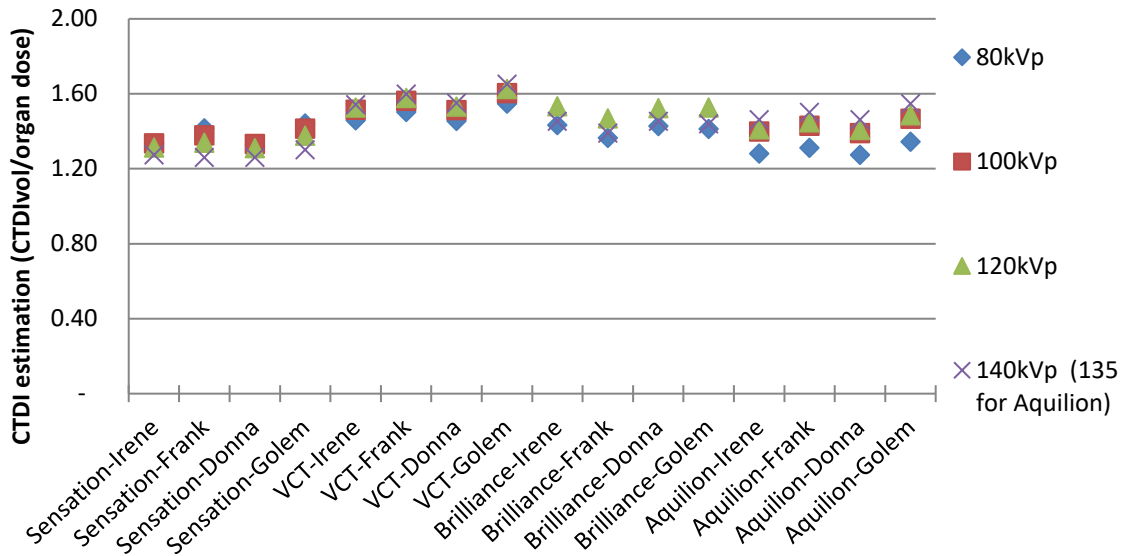


510 **Figure 3. (a) Skin dose and (b) and Eye lens dose under each kV on all four scanners for all four**
patient models on a per 100mAs basis.

515

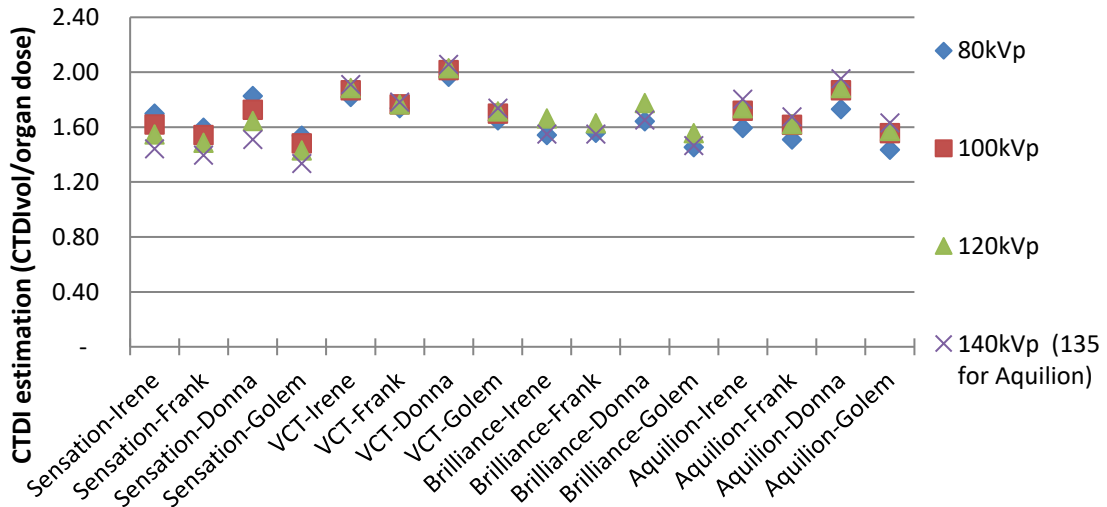
520

Estimation of Skin dose using CTDIvol under each kVp on all four scanners for all four patients



(a)

Estimation of eye lens dose using CTDIvol under each kVp on all four scanners for all four patients

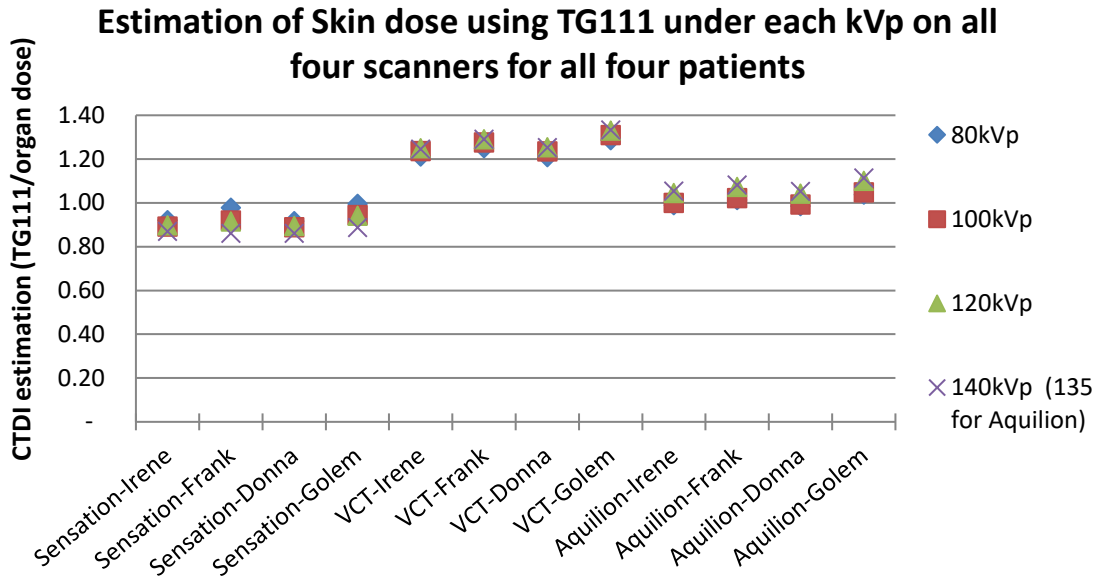


(b)

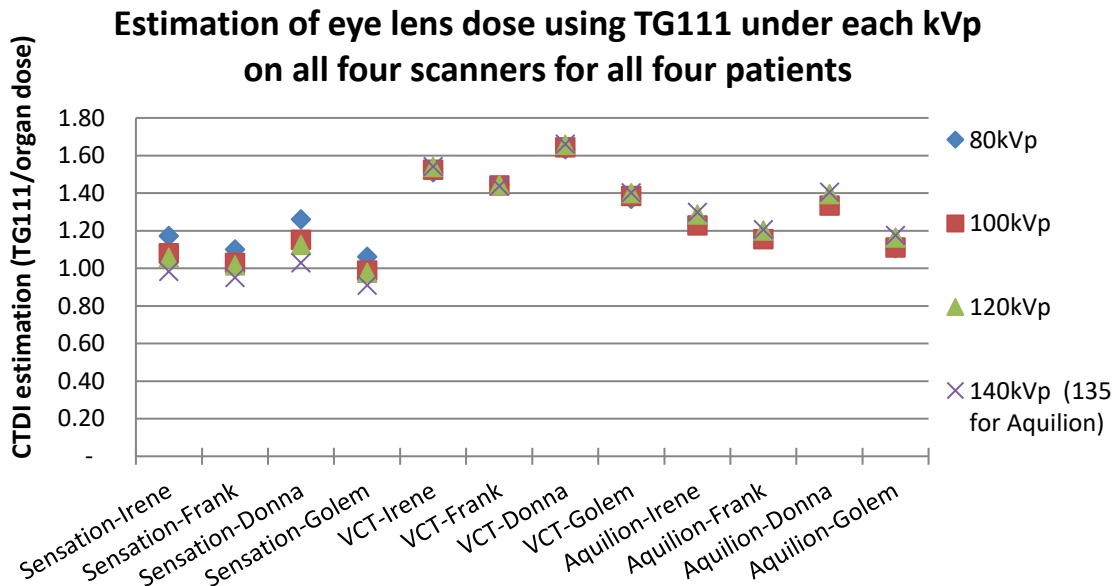
Figure 4. (a) CTDI estimation of skin dose and (b) and eye lens dose under each kV on all four scanners for all four patient models.

525

530



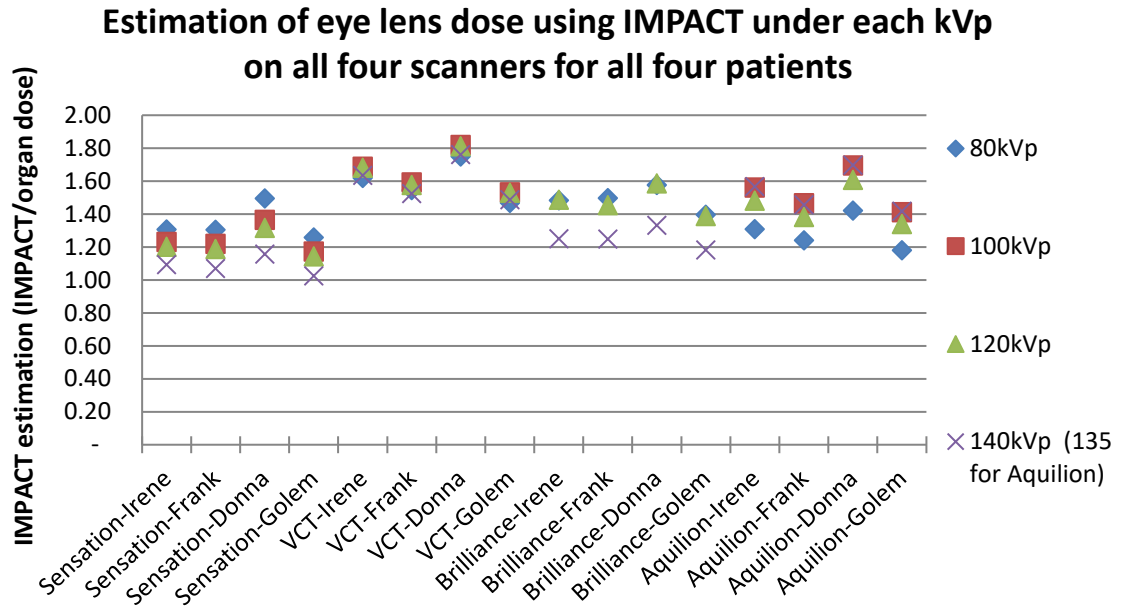
(a)



(b)

535

Figure 5. (a) TG111 estimation of skin dose and (b) eye lens dose under each kV on two scanners for all four patient models.



540 Figure 6. IMPACT estimation of eye lens dose under each kV on all four scanners for all four patient models.